

Satellite Applications of Electromagnetic Cloaking

Stefano Vellucci, Alessio Monti, Mirko Barbuto,
Alessandro Toscano, and Filiberto Bilotti

Abstract—We discuss the possibility to exploit electromagnetic cloaking for enhancing the performances of communication antennas installed on nanosatellite platforms. As a case-study, we consider a CubeSTAR system and show that properly designed metasurfaces can be effectively used to minimize the impact of its deployable payload sensors on both radiation and electrical characteristics of the antennas. The results discussed here pave the way to new strategies for the design of extremely compact nanosatellite platforms equipped with multi-functional antennas and sensors.

Index Terms— Electromagnetic cloaking, satellite antennas, dipole antennas, CubeSat, low observability, metasurfaces, RCS reduction.

I. INTRODUCTION

In the last decade, there has been an increasing interest in the development of cloaking techniques able to make an object completely undetectable in a desired range of frequencies [1]–[7]. Among the different approaches proposed so far, mantle cloaking [8] has emerged as an effective technique characterized by remarkable overall performances, straightforward implementation and ease of fabrication. Moreover, since this technique is based on metasurfaces, the corresponding cloaking devices are lightweight, thin and conformal. At radiofrequencies and microwaves, in particular, the cloaking metasurfaces are realized through patterned metallic sheets able to synthesize the surface impedance required to cancel the scattering from the object to hide.

One of the main advantages of mantle cloaking over other cloaking approaches based, for instance, on transformation electromagnetics [1] lies in the possibility to preserve the electromagnetic functionalities of the covered objects. This peculiar aspect makes this technique particularly appropriate to cloak antennas and sensors as it has been recently proven in [9]–[14] for the case of dipoles and monopoles. The possibility to make an antenna invisible to other radiating systems placed nearby is an important new degree of freedom that can be exploited in highly-dense telecommunication platforms where an ever-increasing number of antennas are packaged together within a limited space.

Manuscript received November 8, 2016; accepted June 18, 2017. Date of publication XXXX XX, 201X; date of current version XXXX XX, 201X.

S. Vellucci, A. Toscano, and F. Bilotti are with the Department of Engineering, “Roma Tre” University, 00146 Rome, Italy (e-mail: stefano.vellucci@uniroma3.it).

A. Monti and M. Barbuto are with the Niccolò Cusano University, 00166, Rome, Italy.

Color versions of one or more of the figures in this communication are available online at <http://ieeexplore.ieee.org>.

Digital Object Identifier XXXXXXXXXXXXX

Satellite platforms represent a significant example where electromagnetic interferences and coupling dramatically limit the functionalities of the on-board communication systems.

Due to the low weight and conformal requirements, the space systems are generally equipped with wire antennas that have the advantage to be deployable after the launch. Other radiator solutions based, for example, on patch antennas would restrict the satellite surface available for energy harvesting with important consequences on the energy autonomy of the entire platform [15].

Moreover, wire antennas are also preferred for their quasi-isotropic radiation pattern [16]. Depending on the type of application, nanosatellites are not always equipped with an alignment control system, due to the low available energy on board, and their spatial orientation in a given moment is totally arbitrary [17]. For this reason, the satellite antenna should exhibit an isotropic gain pattern to minimize the average free-space path loss between the space platform and the ground station. However, the presence of deployable equipment on the satellite, such as external sensors or solar panels, may affect the antenna radiation pattern, severely reducing its degree of isotropy. The metallic passive structures available on the satellite, in fact, can behave either as passive reflectors or directors, causing an unwanted shaping of the radiated beam [18]. This effect makes the link budget between the satellite and the ground station strongly dependent on the satellite orientation. In this context, we emphasize that, due to the limited energy available on the nanosatellite and the significant distance between it and the ground station, even a small reduction in the antenna directivity could affect the telecommunication link.

In this communication, we present a possible solution to this issue based on the use of electromagnetic cloaking to overcome the perturbing effects of deployable objects on the performances of satellite wire antennas. The proposed solution is also suitable to overcome the mutual coupling between different antennas placed on the same space platform [14] introducing, thus, an unprecedented freedom degree in the design of the communication systems of small satellites. To the best of our knowledge, this is the first time that electromagnetic cloaking is employed in a space application and the potential impact of the proposed solution is remarkable due to the challenging telecommunication issues that still affect the small satellites. This new field of application could pave the way to a wide industrial diffusion of cloaking devices.

The paper is organized as follows. In Section II, we describe the case-study adopted in this paper to verify the effectiveness of the proposed idea and discuss the deteriorating effects introduced by the deployable objects on the antenna characteristics. In Section III, we describe the design of mantle cloaks for these objects and confirm, through full-wave simulations, that this solution is able to restore both the radiating and electrical performances of the antenna within its entire operative frequency band. In Section IV, we discuss the robustness of the proposed solution to different configurations and propose new advantageous designs. Finally, in Section V, we briefly summarize the obtained results and discuss some

other applications of mantle cloaking for nanosatellite systems.

II. CASE-STUDY

As a reference scenario to check the effectiveness of the proposed idea, we consider a realistic nanosatellite system based on the CubeSats technology [19].

A CubeSat is a particular type of miniaturized satellite used for space research and made of one or more $10 \times 10 \times 10$ cm³ cubic units (1U). The CubeSats technology provides a standard for the design of low-cost nanosatellites with the aim to increase the accessibility to space and sustain frequent launches. An example of a CubeSat satellite is the so-called CubeSTAR [20], depicted in Fig. 1.

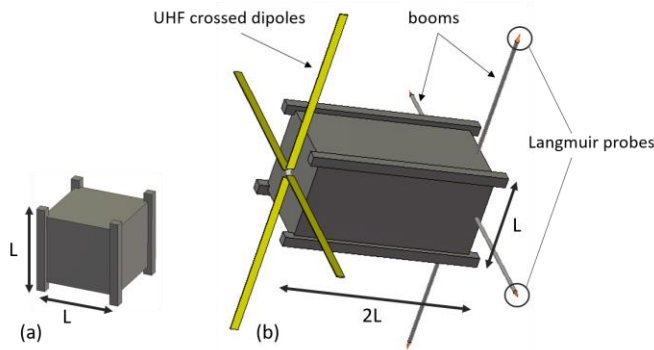


Fig. 1. Sketch of (a) a one unit (1U) CubeSat and (b) a two units (2U) CubeSTAR. The nanosatellite edge is equal to $L = 10$ cm.

Defined as a 2U structure, a CubeSTAR is a space weather nanosatellite whose aim is to measure the absolute electron density in the ionosphere. For this purpose, the satellite exploits deployable metallic sensor booms terminated by Langmuir probes. The radiation system used to communicate with the ground station (for telemetry, tracking, and command) consists of a turnstile crossed-dipoles antenna operating in the UHF amateur satellite band (435-438 MHz) with a central frequency $f_0 = 436.5$ MHz and a channel bandwidth of 25 kHz. As discussed above, this antenna solution is preferred for its quasi-isotropic radiation pattern that guarantees a link budget almost independent on the satellite space orientation. Moreover, a turnstile antenna can be easily designed to radiate the circularly-polarized field required by satellite communications [21].

The 3D radiation diagram of such a turnstile antenna placed on the nanosatellite, obtained through full-wave simulations, is illustrated in Fig. 2(a). It is worth noticing that the radiation diagram is slightly different than the one expected by a free-space turnstile antenna due to the presence of the metallic frame of the satellite that behaves as a director. However, this effect does not compromise the link budget since a quasi-isotropic pattern without any radiation null can be still observed.

Due to the relative small electrical dimensions of the nanosatellite at the antenna operation frequency, the deployable

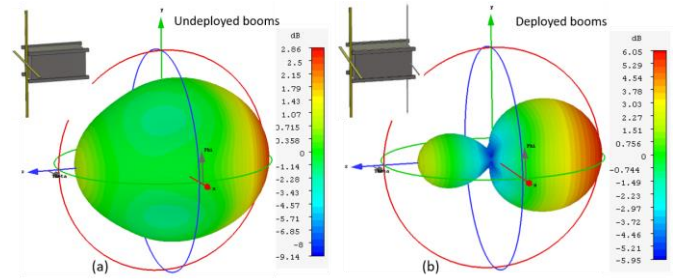


Fig. 2. 3-D gain patterns at f_0 in the case of (a) undeployed and (b) deployed booms.

metallic cylindrical booms (whose radius is $a = 2$ mm) used to measure the ionosphere electron density are placed within the near field of the antenna system. As illustrated in Fig. 2(b), their presence strongly perturbs the radiation diagram of the antenna and dramatically affects its near-field distribution with a consequent change of the antenna input reactance.

In particular, being the payload booms slightly shorter than the dipoles, these structures behave as passive directors for the antenna system, sharpening the radiation diagram and introducing radiation nulls (at $\pm 60^\circ$ ca.). Hence, the link budget is strongly dependent on the satellite orientation and the communication with the ground station is not always guaranteed.

III. MANTLE CLOAK DESIGN AND NUMERICAL RESULTS

In order to significantly reduce the influence of the deployable booms on the antenna performances, we covered each of the four booms with a mantle cloak capable of highly reducing its scattering in the antenna operation bandwidth.

A sketch of a CubeSTAR with cloaked booms is shown in Fig. 3. The design of the cloaking devices applied to the booms has been conducted with the formulas available in [22]-[23] with the aim to achieve the required surface reactance at the central frequency of the antenna. Please note that, since the metallic booms are metallic cylinders slightly shorter than the crossed dipoles, the surface reactance X_s required to reduce their scattering contribution at the central frequency of the CubeSTAR antenna is inductive [24]. Hence, vertical metallic strips are the most suitable geometry to achieve such an average surface reactance [8].

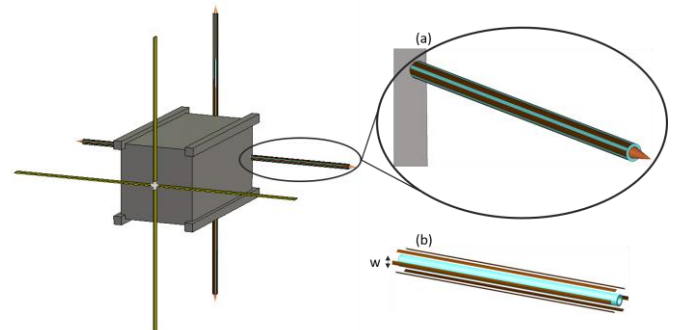


Fig. 3. CubeSTAR with cloaked booms. (a) Detail of the metasurfaces used to achieve cloaking effect and (b) "exploded" components view.

Please note that, since the scattering of electrically thin cylinders is dominated by the TM contribution (*i.e.*, electric field parallel to the cylinder axis) [8], a single-polarized mantle cloak is an effective solution for reducing the booms total scattering.

After a quick numerical optimization, needed to take into account the finite length of the cylinder and its curvature, the cloaks adopted in our setup, shown in Fig. 3, consist of six electrically thin metallic strips ($w = 1.9 \text{ mm}$) patterned on a hollow dielectric cylinder ($\epsilon_r = 8$, outer radius $a_c = 1.5a$, inner radius a). The simple and conformal pattern of the metasurface and the high robustness of the design towards fabrication tolerances [13] allow satisfying all the specific requirements of satellite applications.

Moreover, for the numerical simulations, particular attention has been put in satisfying these specific requirements. Thus, we have considered real properties of ECCOSTOCK® HIK substrates ($\epsilon_r = 8$ and $\tan \delta = 0.002$), which are a series of dielectric materials with low water absorption and low outgassing suitable for space applications.

The radiation and matching properties of the crossed dipoles in presence of the cloaked booms are shown in Fig. 4, Fig. 5 and Fig. 6.

Specifically, in Fig. 4 we compare the far-field gain distribution of the crossed dipoles antenna at the central frequency $f_0 = 436.5 \text{ MHz}$ in the two cases of (a) undeployed sensors booms and (b) deployed cloaked sensor booms. As it can be appreciated, the two 3D distributions are almost equal and the benefits of the cloaks are clearly evident if compared with the 3D distribution in the uncloaked case shown in Fig. 2 (b).

The cloaking effect is confirmed in Fig. 5, where we show the gain patterns of the antenna on the $\phi = 0^\circ$ plane in the undeployed, deployed, and deployed cloaked booms at the central operative frequency and at the lower and upper frequency limits of the antenna operational bandwidth. The patterns are compared with the one of an ideal isotropic antenna. As can be appreciated, the cloaks properly operate within all the antenna bandwidth due to the non-resonant nature of mantle cloaking.

Analogous considerations can be made observing Fig. 6 where we report the magnitude of the reflection coefficient of the antenna in the three cases discussed so far. Note that, due to the inductive reactance introduced by the mantle cloaks, the impedance at the input port of the antenna is restored in the whole operational bandwidth.

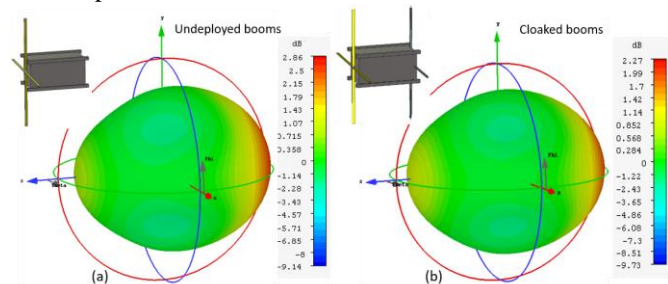


Fig. 4. 3-D gain patterns in the case of (a) undeployed booms, and (b) deployed cloaked booms. The radiation patterns are evaluated at f_0 .

We emphasize that the improvements returned by the cloaks in terms of gain pattern and impedance matching would also allow installing supplemental equipment on the nanosatellite, thanks to the lower energy required by the entire system to maintain the communication link with the ground station.

Finally, we emphasize that the cloaks placed around each metallic boom do not cover the Langmuir sensors (please, see the detail of Fig. 3 (a)). Therefore, also considering the typical materials composing the cloak (traditional dielectrics and metals), no interaction between the cloaks and the sensors is expected. Moreover, it is worth mentioning that the proposed setup also ensures an easy deployability. In fact, since their length is shorter than the satellite main body size, the coated booms can be easily folded along the face of the CubeSTAR during the launch and, then, deployed with the help of torsion-spring hinges.

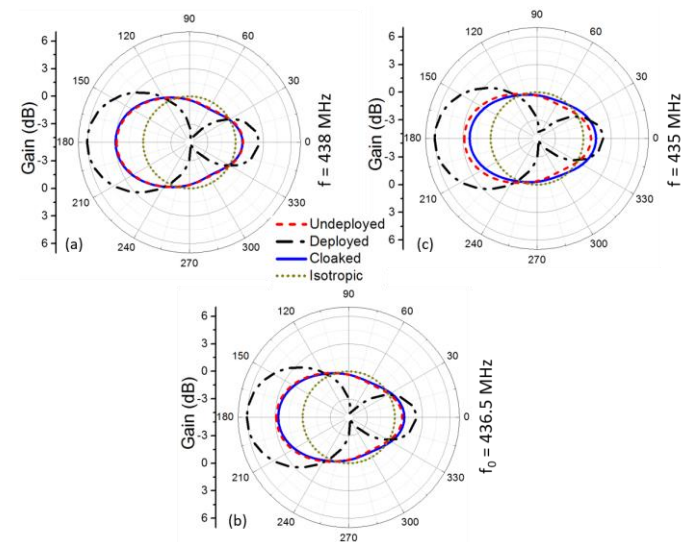


Fig. 5. Gain patterns on the $\phi = 0^\circ$ plane for the case of undeployed (dashed line), deployed (dash-dotted line), and deployed cloaked booms (continuous line) compared to the one of an ideal isotropic antenna (dotted line). Three frequencies are considered: (a) $f_{\max} = 438 \text{ MHz}$, (b) $f_0 = 436.5 \text{ MHz}$ and (c) $f_{\min} = 435 \text{ MHz}$.

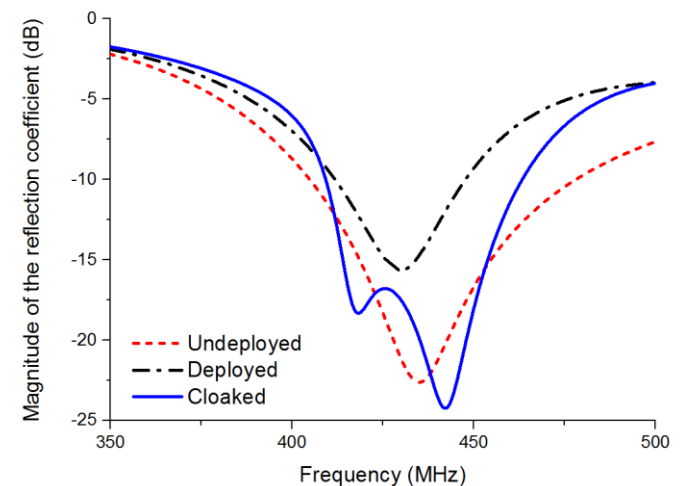


Fig. 6. Magnitude of the reflection coefficient at the input port of the crossed dipoles in the undeployed, deployed, and deployed cloaked booms scenarios.

IV. ROBUSTNESS

In this Section, we analyze the robustness and versatility of the cloaking solution discussed above towards the variations of the geometry of both the antenna and the deployable sensors. We also propose a compact solution based on the use of a 1U nanosatellite instead of the 2U CubeSTAR with the same scientific goal of measuring the electron density in the ionosphere using Langmuir probes.

In Fig. 7(a), we illustrate the first geometry analyzed to evaluate the robustness of the cloaks towards an angular rotation of 35° of the antennas system. As can be noticed, the cloaks are able to perfectly restore the original radiation diagram of the antenna in the undeployed case. The same considerations apply for the shift of the metallic booms towards the nanosatellite edges, as shown in Fig. 7(b).

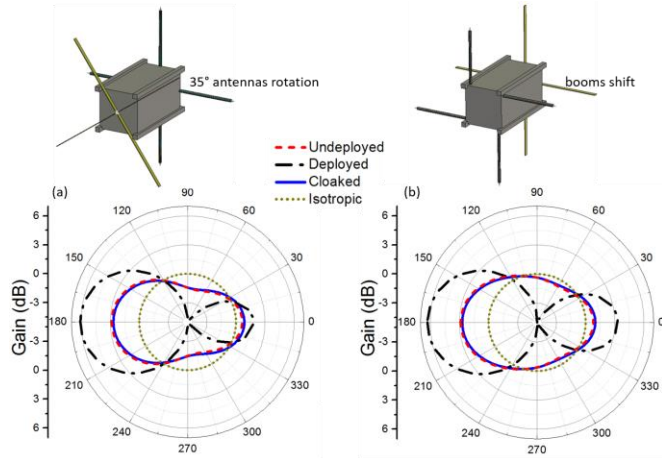


Fig. 7. Gain patterns on the $\phi = 0^\circ$ plane for the case of undeployed (dashed line), deployed (dash-dotted line), and deployed cloaked booms (continuous line) compared to the one of an ideal isotropic antenna (dotted line). (a) 35° antenna rotation; (b) shift of the booms towards the nanosatellite edges.

Finally, we have considered a slightly different scenario, reducing the dimension of the nanosatellite to the one of a 1U (Fig. 8(b)). Compared to the previous one, this solution has the advantage to be more compact, lighter and, consequently, less expensive. However, as appreciable in Fig. 8(a), the gain pattern in case of deployed booms (dash-dotted line) is completely modified compared to the case of undeployed booms (dashed line). This means that, for a large range of possible orientation angle, the communication with the ground station is compromised. In particular, it is worth noticing how the effect of the booms is similar to the one of a reflector according to [18].

Also in this case, electromagnetic cloaking allows overcoming the issue. As shown in Fig. 8(a), by cloaking the booms with the same metasurfaces designed in the previous Section, the gain pattern of the crossed-dipole is completely restored. Furthermore, due to the reduced dimension of the metallic body of the satellite, the gain pattern becomes very similar to the one of a classical free-space crossed dipole antenna.

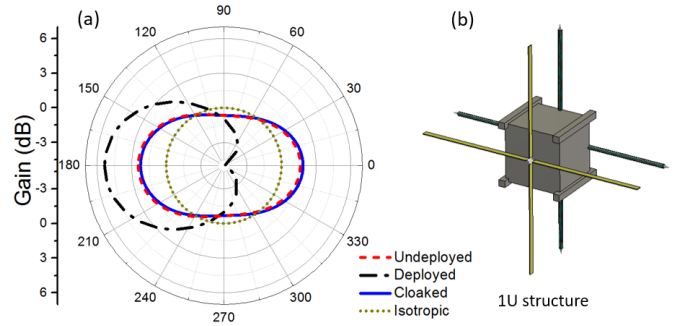


Fig. 8. (a) Gain patterns of a 1U CubeSat on the $\phi = 0^\circ$ plane in the case of undeployed (dashed line), deployed (dash-dotted line), and deployed cloaked booms (continuous line) compared to the one of an ideal isotropic antenna (dotted line); (b) sketch of a 1U CubeSat satellite platform.

Consequently, the use of a 1U CubeSat with cloaked booms allows achieving an almost isotropic radiation pattern and, therefore, a highly-stable communication link between the space system and the ground station.

V. CONCLUSIONS

In this work, we have proposed an innovative solution for satellite communications able to dramatically reduce the interference effects arising between the antennas mounted on the platform and its deployable equipment. By analyzing a typical CubeSat satellite, we have shown how it is possible to make the deployable objects effectively invisible to the antennas within the entire operation bandwidth. This result has been achieved using a simple, conformal and low-cost patterned metallic cover, characterized by a straightforward implementation and ease of fabrication that make this solution particularly suitable for satellite applications.

Finally, we have also shown the robustness and the versatility of the cloaking solution towards geometrical variations on the design of the nanosatellite. In particular, we have highlighted how the cloak functionality is not perturbed if the deployable equipment is placed in the very near field of the antenna.

The proposed setups prove that mantle cloaking technology can be particularly useful in satellite applications, enabling new degrees of freedom in the design of miniaturized space platforms. We also point out that similar cloaking solutions can be employed for multiple-antenna scenarios enabling, thus, unprecedented multi-band solutions in nanosatellite systems.

REFERENCES

- [1] J. B. Pendry, D. Schurig, and D. R. Smith, "Controlling electromagnetic fields," *Sci.*, vol. 312, pp. 1780-1782, 2006.
- [2] P. Alitalo, O. Luukkainen, L. Jylha, J. Venermo, and S.A. Tretyakov, "Transmission-line networks cloaking objects from electromagnetic fields," *IEEE Trans. Antennas. Propag.*, vol. 56, pp. 416-424, 2008.
- [3] A. Alù and N. Engheta, "Achieving transparency with plasmonic and metamaterial coatings," *Phys. Rev. E*, vol. 72, 016623, 2005.
- [4] L. Shen, B. Zheng, Z. Liu, Z. Wang, S. Lin, S. Dehdashti, E. Li, H. Chen, "Large-Scale Far-Infrared Invisibility Cloak Hiding Object from Thermal Detection," *Adv. Opt. Mater.*, vol. 3, pp. 1738-1742, 2015.

- [5] S. Xu, H. Xu, H. Gao, Y. Jiang, F. Yu, J. D. Joannopoulos, M. Soljačić, H. Chen, H. Sun, B. Zhang, "Broadband surface-wave transformation cloak," *Proc. Natl. Acad. Sci. USA* 112, 7635, 2015.
- [6] Y. Yang, H. Wang, F. Yu, Z. Xu, H. Chen, "A metasurface carpet cloak for electromagnetic, acoustic and water waves," *Sci. Rep.*, 6, 20219, 2016.
- [7] Y. Yang, L. Jing, B. Zheng, R. Hao, W. Yin, E. Li, C. M. Soukoulis, H. Chen, "Full-Polarization 3D Metasurface Cloak with Preserved Amplitude and Phase," *Adv. Mater.*, vol. 28, 6866, 2016.
- [8] A. Alù, "Mantle cloak: Invisibility induced by a surface," *Phys. Rev. B*, vol. 80, 245115, 2009.
- [9] A. Alù and N. Engheta, "Cloaking a Sensor," *Phys. Rev. Lett.*, vol. 102, 233901, 2005.
- [10] A. Monti, J. Soric, A. Alù, F. Bilotti, A. Toscano, and L. Vegni, "Overcoming Mutual Blockage Between Neighboring Dipole Antennas Using a Low-Profile Patterned Metasurface," *IEEE Antenn. Wireless Propag. Lett.*, vol. 11, pp. 1414-1417, 2012.
- [11] H. M. Bernety and A. B. Yakovlev, "Reduction of Mutual Coupling Between Neighboring Strip Dipole Antennas Using Confocal Elliptical Metasurface Cloaks," *IEEE Trans. Antennas Propag.*, vol. 63, pp. 1554-1563, 2015.
- [12] Z. H. Jiang, P. E. Sieber, L. Kang, and D. H. Werner, "Restoring Intrinsic Properties of Electromagnetic Radiators Using Ultralightweight Integrated Metasurface Cloaks," *Adv. Funct. Mater.*, vol. 25, 4708, 2015.
- [13] A. Monti, J. Soric, M. Barbuto, D. Ramaccia, S. Vellucci, F. Trotta, A. Alù, A. Toscano, and F. Bilotti, "Mantle cloaking for co-site radiofrequency antennas," *Applied Phys. Lett.*, vol. 108, no. 11, 113502, 2016.
- [14] J. C. Soric, A. Monti, A. Toscano, F. Bilotti, and A. Alù, "Dual-Polarized Reduction of Dipole Antenna Blockage Using Mantle Cloaks," *IEEE Trans. Antennas Propag.*, vol. 63, pp. 4827-4834, 2015.
- [15] A. Nascetti, E. Pittella, P. Teofilatto, and S. Pisa, "High-Gain S-band Patch Antenna System for Earth-Observation CubeSat Satellites," *IEEE Antenn. Wireless Propag. Lett.*, vol. 14, pp. 434-437, 2015.
- [16] C. Balanis, *Antenna Theory: Analysis and Design*. Wiley & Sons, Hoboken, 2005.
- [17] J. Li, M. Post, T. Wright, and R. Lee, "Design of Attitude Control Systems for CubeSat-Class Nanosatellite," *J. Control Sci. Eng.*, 657182, 2013.
- [18] J. Tresvig and T. Lindem, "Investigating the Coupling Effects Between CubeSTAR's Communication Antenna and Deployable Payload Sensors," in *IEEE Antennas Propag. Mag.*, vol. 58, pp. 90-129, 2016.
- [19] W. A. Shiroma, L. K. Martin, J. M. Akagi, J. T. Akagi, B. L. Wolfe, B. A. Fewell, and A. T. Ohta, "Cubesats: A bright future for nanosatellites," *Central European J. Eng.*, vol. 17, no. 1, pp. 24-31, 2011.
- [20] J. Tresvig and T. Lindem, "Cubestar—A nanosatellite for space weather monitoring," in *Proc. 1st IAA Conf. University Satellite Mission Cubesat Workshop*.
- [21] M. Barbuto, F. Trotta, F. Bilotti, A. Toscano, "A Combined Bandpass Filter and Polarization Transformer for Horn Antennas," *IEEE Antenn. Wireless Propag. Lett.*, vol. 12, pp. 1065-1068, 2013.
- [22] Y. R. Padooru, A. B. Yakovlev, P. Y. Chen, and A. Alù, "Analytical modeling of conformal mantle cloaks for cylindrical objects using sub-wavelength printed and slotted arrays," *J. Appl. Phys.*, vol. 112, 034907, 2012.
- [23] A. Monti, J. Soric, A. Alù, A. Toscano, and F. Bilotti, "Anisotropic Mantle Cloaks for TM and TE Scattering Reduction," *IEEE Trans. Antennas. Propag.*, vol. 63, pp. 1775-1788, 2015.
- [24] J. C. Soric, P. Y. Chen, A. Kerkhoff, D. Rainwater, K. Melin, and A. Alù, *New J. Phys.*, vol. 15, 033037, 2013.